Acta Ophthalmologica

Acta Ophthalmologica 2017

MicroRNA regulation in an animal model of acute ocular hypertension

Jiawei Wang,[1,2] Francisco J. Valiente-Soriano,[3] Francisco M. Nadal-Nicolás,[3] Giuseppe Rovere,[3] Shida Chen,[1] Wenbin Huang,[1] Marta Agudo-Barriuso,[3] Jost B. Jonas,[4] Manuel Vidal-Sanz[3] and Xiulan Zhang[1]

[1]Zhongshan Ophthalmic Center, State Key Laboratory of Ophthalmology, Sun Yat-Sen University, Guangzhou, China
[2]Eye Center of Shandong University, The Second Hospital of Shandong University, Jinan, China
[3]Department of Ophthalmology, University of Murcia and Murcian Institute of Biosanitary Research-Hospital Arrixaca (IMIB-Arrixaca), Murcia, Spain
[4]Department of Ophthalmology, Medical Faculty Mannheim, Heidelberg University, Heidelberg, Germany
[Correction added on 29 August 2016, after first online publication: The first and second affiliations were wrongly swapped and have been corrected in this version.]

ABSTRACT.

Purpose: **To analyse miRNA regulation in a rat model of acute ocular hypertension (AOH).**

Methods: **Acute ocular hypertension (AOH) was induced in the left eye of adult albino rats by inserting a cannula connected with a saline container into the anterior chamber. The contralateral eye served as a control. Seven days later, animals were killed. Retinas were used either for quantitative analysis of retinal ganglion cells (RGCs) and microglial cells or for miRNA array hybridization, qRT-PCR and Western blotting.**

Results: **Anatomically, AOH caused axonal degeneration, a significant loss of RGCs and a significant increase in microglial cells in the ganglion cell layer. The miRNAs microarray analysis revealed 31 differentially expressed miRNAs in the AOH versus control group, and the regulation of 12 selected microRNAs was further confirmed by qRT-PCR. Bioinformatic analysis indicates that several signalling pathways are putatively regulated by the validated miRNAs. Of particular interest was the inflammatory pathway signalled by mitogen-activated protein kinases (MAPKs). In agreement with the *in silico* analysis, p38 MAP kinase, tumour necrosis factor-alpha (TNF-α) and iNOS proteins were significantly upregulated in the AOH retinas.**

Conclusions: **Acute IOP elevation led to changes in the expression of miRNAs, whose target genes were associated with the regulation of microglia-mediated neuroinflammation or neural apoptosis. Addressing miRNAs in the process of retinal ischaemia and optic nerve damage in association with high IOP elevation may open new avenues in preventing retinal ganglion cell apoptosis and may serve as target for future therapeutic regimen in acute ocular hypertension and retinal ischaemic conditions.**

Key words: acute glaucoma model – acute ocular hypertension – microRNA – optic nerve damage – retinal ganglion cells – retinal ischaemia – retinal microglia

Acta Ophthalmol. 2017: 95: e10–e21

doi: 10.1111/aos.13227

Introduction

Acute angle-closure glaucoma results in an increase in the intra-ocular pressure (IOP) which may temporarily exceed the retinal perfusion pressure, and this may result in retinal ischaemia, optic nerve damage and retinal ganglion cell (RGC) death (Selles-Navarro et al. 1996; Lafuente et al. 2002). Although a number of mechanisms and molecules have been found to be potentially associated with the aetiology of retinal/optic nerve damage in acute angle-closure glaucoma, the main causes are, so far, elusive (Almasieh et al. 2012). In particular, the role that microRNAs (miRNA) may play in the development of retinal damage is yet unclear (Genini et al. 2014). miRNAs are an evolutionarily conserved class of non-coding small RNAs that have a length of approximately 19~23 nucleotides and play a crucial part in the post-transcriptional regulation of gene expression (Bartel 2004, 2009; Bentwich et al. 2005; Lewis et al. 2005). miRNAs derive from long endogenous transcripts and undergo several processing steps to yield mature miRNAs. The mature miRNAs regulate the gene expression through binding the 3′-untranslated region (3′-UTR) of its target gene, resulting in either reduced protein translation or degradation of the mRNA (Bartel 2004, 2009; Bentwich et al. 2005; Lewis et al. 2005). Considerable abundance of

miRNAs has been found in the retina. Previous studies have indicated the essential roles of miRNAs in the development, survival and normal function of the retina (Almasieh et al. 2012; Maiorano & Hindges 2012). miRNAs also play a key role in the regulation of polarization of microglial cells and have thus an effect on the progress of retinal disorders (Andreeva & Cooper 2014).

An abnormal expression or activity of miRNAs in the retina has been described in a variety of ophthalmic diseases in human patients and in animal models. These disorders include primary vitreo-retinal lymphoma, uveitis, ocular adnexal lymphoma or diabetic retinopathy among other conditions (Kovacs et al. 2011; Dunmire et al. 2013; Funari et al. 2013; Hother et al. 2013; Kutty et al. 2013; Tanaka et al. 2014; Tuo et al. 2014). Recently, it has been described the implication of miRNAs in the maintenance of the trabecular meshwork, an organ of high relevance in high-tension glaucoma (Saccà et al. 2016). Since an association between miRNA regulation and acute ocular hypertension (AOH) has not yet been examined, we purposed here to analyse whether retinal miRNAs were regulated in a rat model of acute increase in IOP (AOH; acute ocular hypertension) and if so, to study which signalling pathways and biological process may be affected using *in silico* prediction tools.

Materials and Methods

Animal handling

The study was approved by the Committees of Animal Care of the Sun Yat-Sen University (Guangzhou, China) and the University of Murcia (Murcia, Spain), and all experimental procedures were performed in accordance with the European Union Directive 2010/63/EU for animal experiments and the Association for Research in Vision and Ophthalmology (ARVO) statement for the use of animals in ophthalmologic research. All experiments were performed in adult female Sprague Dawley rats (200–250 g body weight). Animals had free access to food and water and were kept in an environmentally controlled room with an alternating 12-hr/12-hr light/dark cycle. Animals were euthanized with an overdose of sodium pentobarbital injected intraperitoneally (Dolethal, Vetoquinol®, Especialidades Veterinarias, S.A., Madrid, Spain).

Acute ocular hypertension induction

This technique has already been described in detail previously (Huang et al. 2007, 2008; Zhang et al. 2009; Chi et al. 2014). Briefly, animals were anesthetized using a mixture of xylazine (10 mg/kg body weight, Rompun; Bayer, Kiel, Germany) and ketamine administered intraperitoneally (60 mg/kg body weight, Ketolar; Pfizer, Alcobendas, Madrid, Spain). Additionally, topical anaesthesia was achieved with 0.5% proparacaine hydrochloride eye drops (Alcon Co., Fort Worth, TX, USA). A 30-gauge infusion needle connected to a 500-ml plastic bottle of sterile saline was placed into the anterior chamber of the left eye. By lifting the infusion bottle to a height of 150 cm above the level of the eye, IOP was elevated to 110 mmHg for a period of 60 min. Intra-ocular pressure (IOP) was measured using a Tono-Pen (Tono-Pen; Medtronic Co., Dublin, Ireland), following previously described methods (Salinas-Navarro et al. 2010; Ortín-Martínez et al. 2015; Valiente-Soriano et al. 2015a,b). Care was taken not to injure the lens and the iris during the experiment, and animals with an impaired lens were excluded from the study. After 60 min, the infusion needle was removed from the anterior chamber. The right retinas of these animals served as control group. All animals were killed 7 days after the induction of IOP elevation; such a survival interval was chosen because, as shown here and in accordance with previous studies, at this time–point, AOH causes RGC death and microglial activation (Leung et al. 2009; Zhang et al. 2009; Liu et al. 2012b). The number of retinas used in each analysis is detailed in results.

Retinal dissection, immunodetection and imaging

Animals were perfused transcardially with 4% paraformaldehyde in phosphate buffer 0.1 M after a saline rinse. Then, retinas were dissected as whole mounts (Nadal-Nicolás et al. 2012; Rovere et al. 2015) and immunodetected following previously described methods (Salinas-Navarro et al. 2010; Nadal-Nicolás et al. 2012). Microglial cells (Iba1, Galindo-Romero et al. 2013) and RGC (Brn3a Nadal-Nicolás et al. 2014) or RGCs (Brn3a) and their intraretinal axons (pNFH, Parrilla-Reverter et al. 2009) were double-immunodetected. Primary antibodies were rabbit anti-Iba-1 (1:500 dilution; Dako; Rafer, Zaragoza, Spain), mouse IgG1 anti-pNFH (1:200 dilution, Clone RT-97; Serotec, Bionova, Spain) and goat anti-Brn3a (1:750 dilution; C-20, Santa Cruz Biotechnology, Heidelberg, Germany). Iba1 is expressed by microglial cells (Galindo-Romero et al. 2013): Brn3a is expressed by the vast majority of the general population of RGCs (approximately 97%), except the melanopsin-expressing RGCs and one half of the ipsilaterally projecting RGCs (Nadal-Nicolás et al. 2012, 2014, 2015). The monoclonal antibody RT97 recognizes the phosphorylated heaviest subunit of the neurofilament triplet (pNFH), and its abnormal expression is an index of axonal injury (Vidal-Sanz et al. 1987; Villegas-Pérez

Table 1. miRNAs selected for qRT-PCR validation.

miRNA	Accession number	Amplicon size(bp)	Sequence
rno-miR-1-3p	MIMAT0003125	22	UGGAAUGUAAAGAAGUGUGUAU
rno-miR-190a-5p	MIMAT0000865	22	UGAUAUGUUUGAUAUAUUAGGU
rno-miR-539-5p	MIMAT0003176	22	GGAGAAAUUAUCCUUGGUGUGU
rno-miR-17-5p	MIMAT0000786	23	CAAAGUGCUUACAGUGCAGGUAG
rno-miR-215	MIMAT0003118	22	AUGACCUAUGAUUUGACAGACA
rno-miR-628	MIMAT0012836	22	AUGCUGACAUAUUUACGAGAGG
rno-miR-22-3p	MIMAT0000791	22	AAGCUGCCAGUUGAAGAACUGU
rno-miR-350	MIMAT0000604	24	UUCACAAAGCCCAUACACUUUCAC
rno-miR-336-5p	MIMAT0000576	21	UCACCCUUCCAUAUCUAGUCU
rno-miR-93-5p	MIMAT0000817	23	CAAAGUGCUGUUCGUGCAGGUAG
rno-miR-532-3p	MIMAT0005323	22	CCUCCCACACCCAAGGCUUGCA
rno-miR-124	MIMAT0000828	20	UAAGGCACGCGGUGAAUGCC

et al. 1988; Parrilla-Reverter et al. 2009). Secondary detection was carried out with Alexa Fluor-conjugated antibodies (donkey anti-rabbit Alexa 594, donkey anti-goat Alexa 488 and goat anti-mouse IgG1 Alexa 488, all diluted at 1:500; Molecular Probes Thermo-Fisher, Madrid, Spain). After immunodetection, retinas were mounted on glass slides with the vitreal side up and covered with antifading solution (Nadal-Nicolás et al. 2015).

Photographic reconstructions of whole-mounted retinas were obtained under an epifluorescence microscope (Axioscop 2 Plus; Zeiss Mikroskopie, Jena, Germany) equipped with a computer-driven motorized stage (ProScan H128 Series; Prior Scientific Instruments, Cambridge, UK) according to previously described methods (Vidal-Sanz et al. 2012, 2015a,b). Then, the individual frames (154/retina) were reconstructed and further analysed. The total number of Brn3a$^+$RGCs was automatically quantified using the Image-Pro Plus (IPP 5.1, Media Cybernetics, Silver Spring, MD, USA) software, as reported (Nadal-Nicolás et al. 2012). With these quantitative data, isodensity maps of Brn3a$^+$ RGCs were constructed using a graphing software (SIGMAPLOT© R) as reported (Vidal-Sanz et al. 2012, 2015a,b). For quantitative analysis of the Iba-1$^+$ microglia in the ganglion cell layer, 12 rectangular areas (0.36 × 0.24 mm) at a magnification of ×100 were taken from concentric zones of each retina, three per quadrant at equidistant distances from the optic disk. The total number of microglial cells obtained in these areas was averaged to obtain a mean cell density per retina. Then, the total numbers of microglial cells in the whole-mounted retina were estimated by multiplying the mean cell density times the total area of the retina.

miRNA microarray analysis

Retinas were freshly dissected and immediately frozen. Total retinal RNA was extracted using the Trizol reagent (Life Technologies Invitrogen Co., Carlsbad, CA, USA). Quantity and purity of the RNA were assessed using the DW-K5500 micro-spectrophotometer (Drawell International Technology Co., Ltd. Shanghai, China). A ratio of 260/A280 ≥ 1.5 and a ratio of A260/A230 ≥ 1 indicated an acceptable RNA purity, and an RNA Integrity Number (RIN) value of ≥7 as assessed by the Agilent 2200 RNA assay (Agilent Technologies, Santa Clara, CA, USA) indicated an acceptable RNA integrity. The screening of the miRNA expression profiling was performed using the commercial Rat miRNA Microarray 1 × 12K kit according to the manufacturer's protocol (RiboBio Ltd., Guangzhou, China). All analyses and annotations were based on the miRbase database release 21.0. To reduce the errors of the

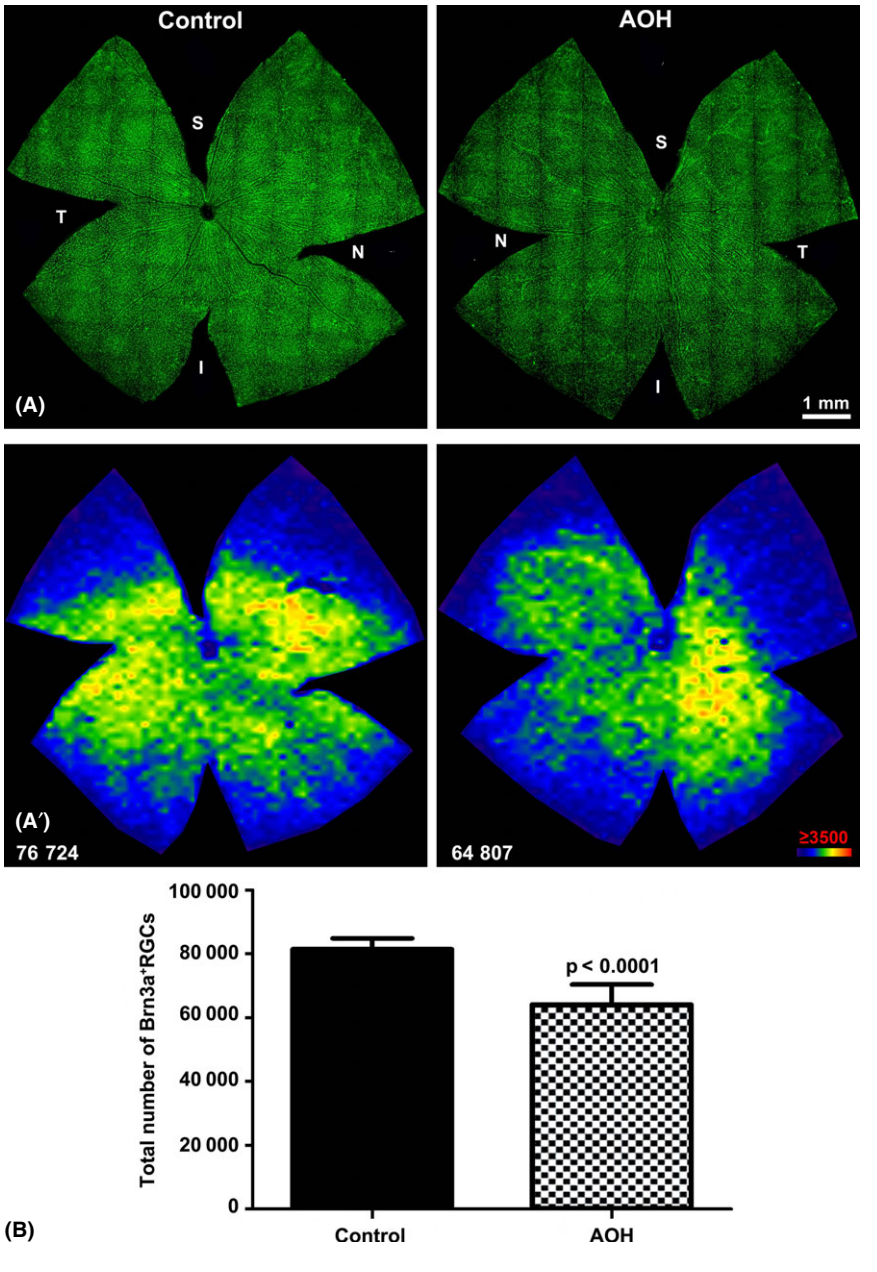

Fig. 1. Seven days after induction of AOH, there is a diffuse loss of retinal ganglion cells. (A-A') Retinal photomontages showing Brn3a$^+$RGCs in a control (A, left) and an experimental (A, right) retina and their isodensity maps (A'). Maps in this figure show that in control retinas, RGCs are denser in the medial–central retina, being densest above of the optic nerve. A diffuse loss of RGCs is observed after AOH. At the bottom of each map is shown the number of RGCs quantified in its corresponding retina. Density colour scale is shown at the bottom of panel A' right and goes from 0 RGCs/mm^2 (purple) to ≥3500 RGCs/mm^2 (red). (B) Bar graph showing the mean ± standard deviation of RGCs in control and AOH retinas (n = 6/group). The loss of RGCs in the AOH retinas is significant compared to control (t-test, p-value <0.0001). AOH, acute ocular hypertension; S, superior; N, nasal; T, temporal; I, inferior.

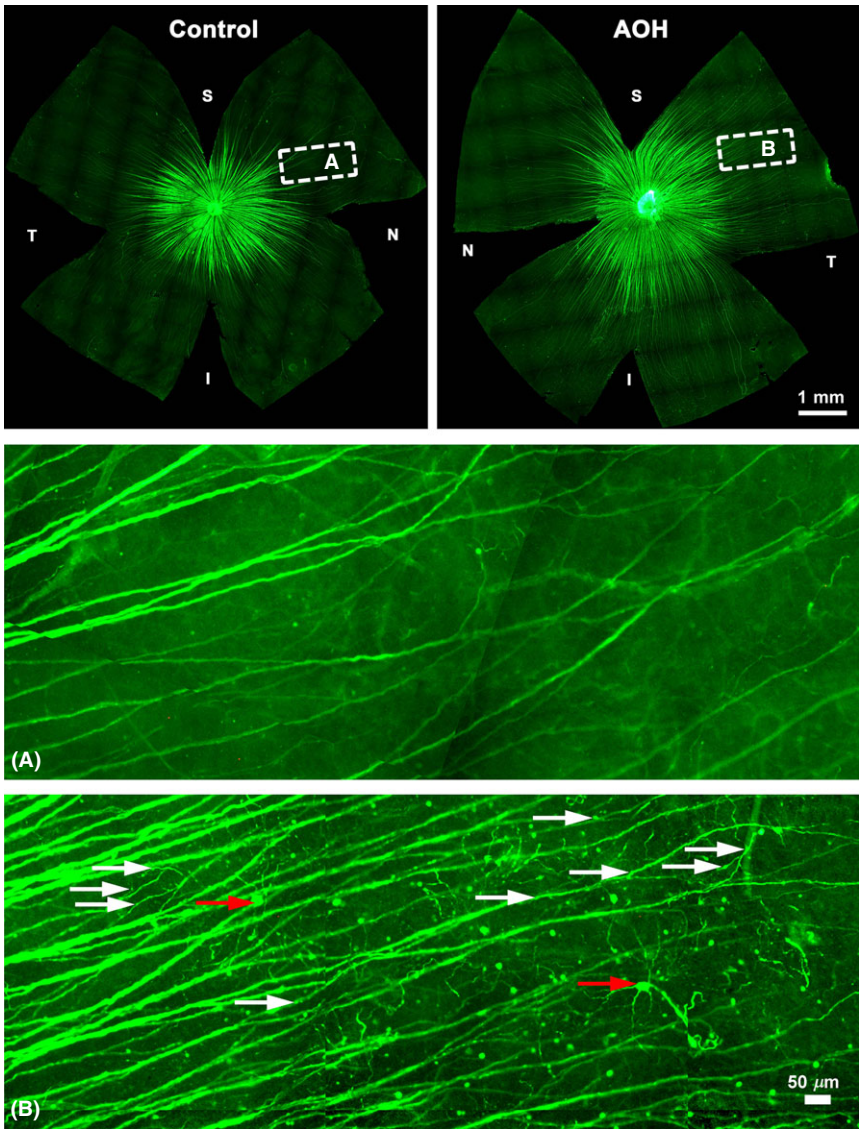

Fig. 2. Acute ocular hypertension (AOH) causes the degeneration of RGC intraretinal axons. Retinal photomontages showing pNFH$^+$ intraretinal RGC axons in a control and an experimental retina. Below each photomontage is shown a magnification of the squared areas (A, B). In control retinas, pNFH expression is restricted to the middle and central retina while after AOH extends to the periphery. The abnormal pNFH expression in the AOH retinas depicts intensely stained RGCs (red arrows) as well as beaded axons (white arrows), showing the typical features of AOH-induced retrograde axonal degeneration.

microarray analysis, three paired samples were measured and each experimental condition was independently repeated three times. In each of these three biological repetitions, three technical replicas were made. All biological replicates were pooled and calculated to identify differentially expressed miRNAs. A given miRNA was considered differentially expressed in AOH retinas when its fold change was a factor of 2 or more compared to control retinas with a statistical p-value of <0.05. To directly display the correlations among the replicates and sample conditions, a cluster analysis was performed which was visualized by a *Z*-score.

qRT-PCR validation

Total retinal RNA was extracted as above. Retrotranscription primers (steem loop) and qPCR primers (forward and reverse) for each miRNA were designed by RiboBio (Guangzhou, China; Punj et al. 2010). Two micrograms of total RNA was reversely transcribed with moloney murine leukaemia virus reverse transcriptase (Promega, Madison, WI, USA). Quantitative PCRs were performed with Platinum SYBR Green qPCR SuperMix-UDG reagents (Invitrogen, Carlsbad, CA, USA) using the PRISM 7900HT system (Applied Biosystems, Carlsbad, CA, USA). U6 snRNA was used as endogenous control for the quantification of miRNAs (Liu et al. 2012a). Each sample was measured three times. The selected miRNAs are listed in Table 1.

In silico pathway analysis

To comprehensively predict the target genes of the validated miRNAs, TARGETSCAN (www.targetscan.org/), MIRWALK (http://zmf.umm.uni-heidelberg.de/apps/zmf/mirwalk2/) and MIRDB (http://mirdb.org/miRDB/) free databases were used. Only their intersection was regarded as target genes. Each gene was assigned to an appropriate signalling pathway according to its main cellular function. The Database for Annotation, Visualization and Integrated Discovery 6.7 (DAVID; https://david.ncifcrf.gov/) was used for gene ontology analysis. Signalling pathway analysis was performed using the microarray gene pathway annotations acquired from Kyoto Encyclopedia of Genes and Genomes (KEGG, http://www.genome.jp/kegg/). Pathways with a p-value of <0.05 were chosen as significantly regulated. All statistical analyses were performed applying Fisher's exact test, and the p-values were adjusted using the false discovery rate algorithm for the microarray analysis of miRNAs (Zhang et al. 2012).

Western blotting

Retinas were fresh-dissected and homogenized in RIPA lysis buffer (Beyotime Institute of Biotechnology, Haimen, China) supplemented with 100 mM PMSF. Protein concentration was assessed using BCA Protein Assay Kit (Beijing CoWin Bioscience Co., LTD. Beijing, China). Samples containing equal amounts of protein (20–50 μg) were separated in 8 or 12% sodium dodecyl sulphate–polyacrylamide gel electrophoresis (SDS-PAGE) and then transferred to PVDF membranes. Proteins were blocked with 5% non-fat milk in PBS for 1 hr and then incubated overnight at 4°C with the following primary antibodies: rabbit antiphosphorylated-p38 MAP kinase (Thr180/Tyr182, 1:500 dilution. sc-17852-R),

rabbit antitotal p38 MAP kinase (1:500; sc-7149), goat anti-tumour necrosis factor-alpha (TNF-α) (1:500; sc-1350) and rabbit anti-iNOS (1:800; sc-650) purchased from Santa Cruz Biotechnologies. Secondary detection was performed with horseradish-conjugated antibodies (1:5000 or 1:10 000, from Beijing Biosynthesis Biotechnology). Signal was visualized using an enhanced chemiluminescence kit (Millipore,-Jaffrey, NH, USA). Membranes were exposed to X-ray films that were scanned using a molecular dynamic densitometer (Scion, Frederick, MD, USA). Then Quality One software (Bio-Rad, Philadelphia, PA, USA) was used for the densitometric analysis. β-Actin (1:500, sc-130656; Santa Cruz Biotechnologies) was used as loading control.

Statistics

Statistical analysis was performed using the programs of SPSS (version 22.0; SPSS Inc., Chicago, IL, USA) and GRAPH PAD PRISM (version 5.0 Graph Pad Inc., La Jolla, CA, USA). The data are presented as mean ± standard deviation. Acute ocular hypertension (AOH) and control groups were compared with each other using the Student's *t*-test. A p value of <0.05 was considered to be statistical significant.

Results

RGC loss, axonal degeneration and microglial activation

Examination of the retinal whole mounts 7 days after the induction of AOH revealed that the density of RGCs was significantly lower in the Acute ocular hypertension (AOH) retinas compared to the control ones. In control retinas, the total number of $Brn3a^+$ RGCs was 81 451 ± 3383 (mean ± standard deviation; $n = 6$), while in AOH retinas, this number decreased to 64 143 ± 6229 ($n = 6$), which accounts for a loss of approximately 21.3% of RGCs (Fig. 1).

In control retinas, $pNFH^+$ intraretinal axons were constricted to the central and middle regions of the retina and had a rectilinear morphology (Fig. 2, 2A). In contrast, in the AOH retinas, the pNFH signal extended to the periphery of the retinas, with the presence of abnormal expression of pNFH within cell bodies and primary dendrites of RGCs. In addition, there were many intra-axonal deposits of pNFH shaped like small varicosities and rosary beads (Fig. 2B). All these findings are compatible with an axonal injury and have been previously observed after axotomy (Vidal-Sanz et al. 1987; Villegas-Pérez et al. 1988; Parrilla-Reverter et al. 2009) or ocular hypertension (Salinas-Navarro et al. 2009, 2010; Vidal-Sanz et al. 2012).

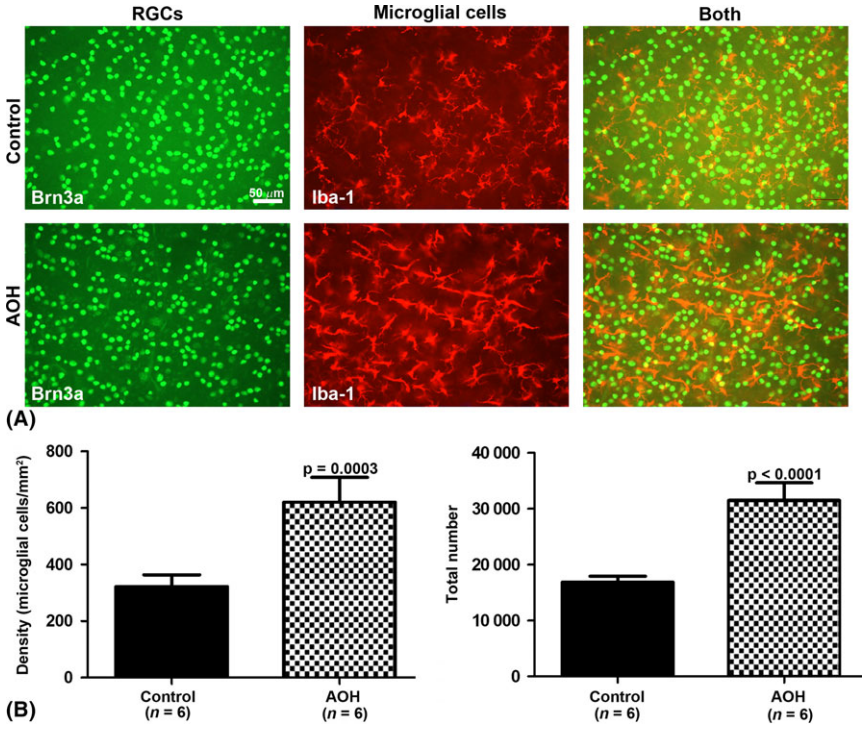

Fig. 3. Increased number of microglial cells in the ganglion cell layer after acute ocular hypertension (AOH). (A) Magnifications from flat-mounted retinas immunodetected for Brn3a (RGCs) and Iba1 (microglial cells) and focused on the ganglion cell layer. In control retinas, microglial cells are ramified and evenly distributed. In AOH retinas, microglial cells are amoeboid, less ramified and more abundant. (B) Graphs showing the mean density (left) and the calculated total number (right) ±standard deviation of microglial cells in control or AOH retinas (see Methods for details). The number of microglial cells in the AOH retinas is significantly higher than in control retinas ($n = 6$/group; *t*-test, pvalue <0.0003).

Microglial cells in control retinas were present as 'resting' ramified microglia with several processes. However, in the AOH retinas, microglial cells changed to an amoeboid shape indicative of their activated state (Fig. 3A; Jonas et al. 2012; de Hoz et al. 2013). Furthermore, in the ganglion cell layer of the AOH retinas (Fig. 3B), the density of microglial cells was almost twofold of control retinas.

miRNA regulation

When the AOH eyes (study group) were compared with the contralateral eyes without IOP change (control group), we detected 31 miRNAs which were differentially expressed, that is the degree of expression differed by a factor of ≥2. In the study group, among these 31 miRNAs, 9 miRNAs were upregulated and 22 miRNAs were downregulated (Fig. 4). The validity of the microarray analysis was verified by qRT-PCR, and the regulation trend for all validated miRNA was in correspondence with the results from the microarray profiling (Fig. 5). Of note, we performed qRT-PCR of miR-124 because, even though it was not regulated in the array analysis, it is expressed by microglial cells (Caldeira et al. 2014) and upregulated in a model of oxygen–glucose deprivation (Kong et al. 2014). As seen in Fig. 5, there was no change of miR-124 between control and AOH retinas. This is further discussed below.

In silico prediction of regulated pathways: Upregulation of proinflammatory proteins

Three prediction-free databases of microRNA targets (TARGETSCAN, MIRWALK and MIRDB) were applied to

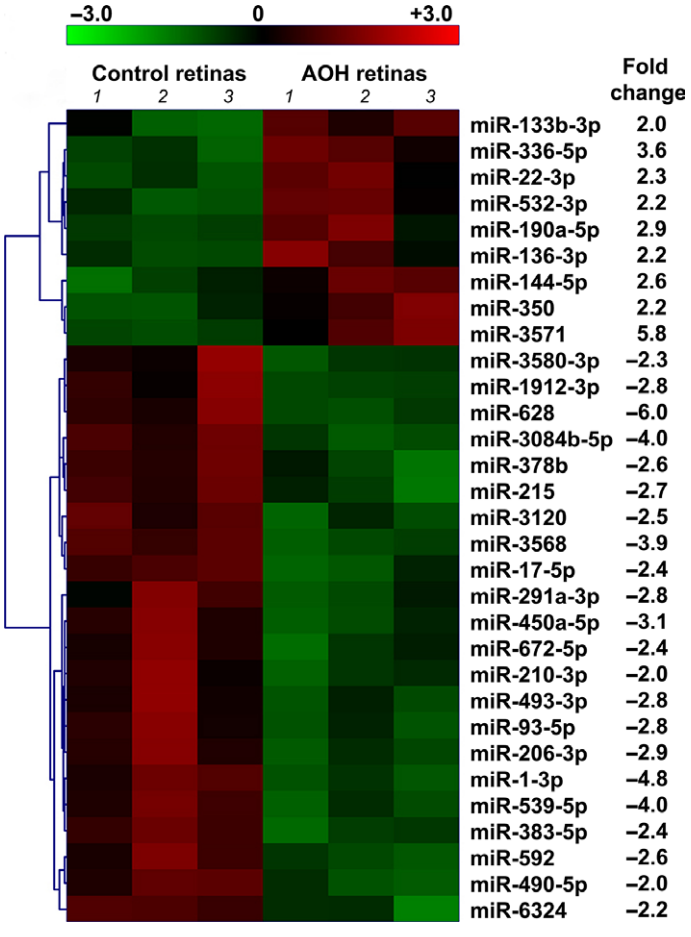

Fig. 4. Heat map of miRNA expression profiles. Thirty-one miRNAs significantly changed between the AOH and control retinas. Significant upregulation or downregulation of each miRNA was determined as fold changes >2.0 and the values are shown at the right. Red indicates high expression level, and green indicates low expression level.

disclose the integrated miRNA-target and gene ontology analysis. After, based on biological process and molecular function, the resulting data were used to uncover the miRNA-Gene Regulatory Network (Figs 6 and 7). This analysis revealed that every miRNA had multiple gene targets and each target gene was regulated by more than one miRNA. In a next step, we performed a pathway analysis using DAVID and KEGG platforms, to clarify the putative pathways in which the miRNAs were involved (Tables 2 and 3). The upregulated miRNAs were ascribed to five functional clusters and the downregulated miRNAs to nine functional clusters (Tables 2 and 3). For a subsequent analysis, we focused on the MAPK pathway which had 18 genes that, according to the bioinformatics analysis, may be targets of the regulated miRNAs. Thus, we performed Western blotting of three proteins linked to the MAPK pathway, stress and inflammation. As shown in Fig. 8, AOH upregulated the stress kinase p38 and the production of inflammatory proteins iNOS and TNF-α. These upregulations concord with the observed increase and activation of microglial cells.

Discussion

In our experimental study on rats with an acutely elevated IOP to supradiastolic pressure levels for a period of one hour, a significant loss in retinal ganglion cells was associated with an activation of retinal microglial cells and an upregulation or downregulation of 31 miRNAs. Some of these miRNAs were involved in various biological processes including regulation of neuron apoptosis and inflammatory pathways.

The findings obtained in our study agree with results of previous investigations showing that a short-term increase in IOP to values of 100 mmHg or higher can lead to marked retinal damage with resulting loss in RGCs and axonal degeneration (Selles-Navarro et al. 1996; Naskar et al. 2002; Zhang et al. 2009; Liu et al. 2012b). Our results are also in agreement with previous studies showing that damage to RGCs is associated with an activation of retinal microglial cells (Salvador-Silva et al. 2000; Sobrado-Calvo et al. 2007; Gallego et al. 2012; Liu et al. 2012b; de Hoz et al. 2013; Abbott et al. 2014; Rojas et al. 2014). In addition, our miRNA analysis revealed, through a bioinformatics analysis, a cluster of signalling pathways predicted to be regulated by the differentially expressed miRNAs. Various cellular activities in mammals including innate immunity, cell proliferation, differentiation, apoptosis or survival, and inflammation can be regulated by the top signalling pathways.

The mitogen-activated protein kinases (MAPKs) signalling pathways were enriched signalling pathways possibly regulated by the differentially expressed miRNAs, for instance miR-350/MAPK14, miR-539/MAP3K8, miR-93/MAPK9. The MAPKs pathways include the c-Jun NH2-terminal kinase, p38 MAP kinase and extracellular signal-regulated kinase and are involved in a wide variety of cellular processes. For instance, in vascular tissue, it has been shown that the activation of the PI3K/Akt/mTOR survival signalling pathway with a concomitant suppression of the p38 MAPK proapoptotic pathway protects the endothelium against stress-induced apoptosis (Joshi et al. 2005). Furthermore, the compromised MAPKs pathways contribute to the pathology of many neurodegenerative diseases (Kim & Choi 2015). Our findings showed accelerated p38 MAP kinase in the AOH eyes. Activated p38 MAP kinase causes the release of inflammatory factors, whose accumulation induces a cascade of events leading to inflammation and RGC death. The differentially expressed miRNAs and abnormally activated p38 MAP kinase provides a potential way to suppress the inflammation and prevent RGC damage caused by acute IOP elevation.

The differentially expressed miRNAs are assumed to influence the function of microglia by regulating specific cell signalling pathway, such

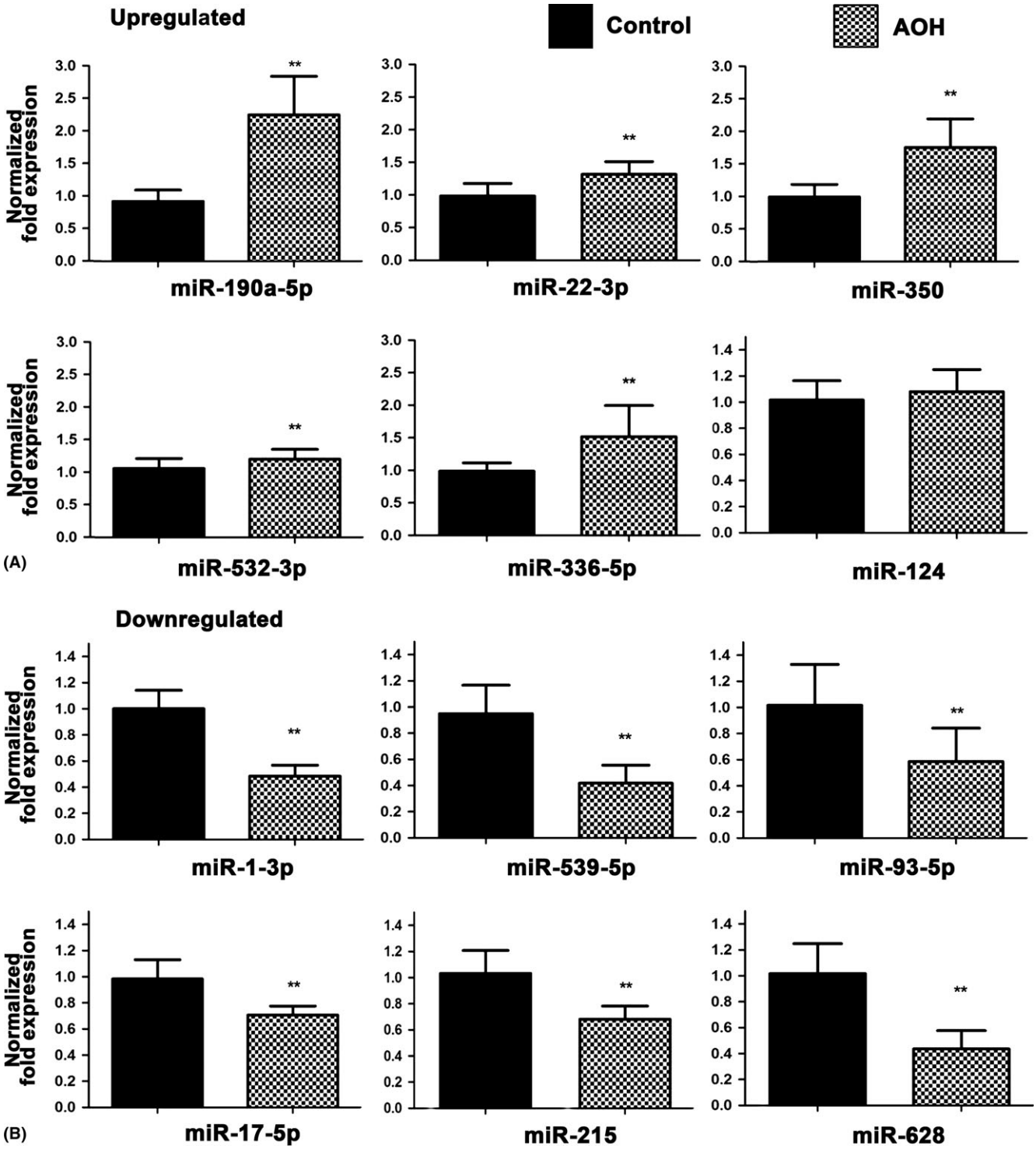

Fig. 5. qRT-PCR validation of regulated miRNAs. (A) Upregulated miRNAs. (B) Downregulated miRNAs. Data are presented as the mean ± standard deviation (n = 5 retinas/group, **p < 0.01. AOH, acute ocular hypertension.

as chemokine signalling pathway and TGF-beta signalling pathway. The prevailing phenotype of retinal microglia is the resting phenotype M2, which is able to release high levels of anti-inflammatory cytokines, associated with recovery, repair and neuroprotection in retinal development and various other retinal disorders. Following injuries, retinal microglia cells change into an activated phenotype M1, which can produce proinflammatory factors and contribute to retinal dysfunctions. Retinal microglial cells M1 and M2 can transform from each other upon different types of stimulation, a process known as 'polarization'. Several miRNAs have been shown to be important regulators of microglial polarization and play a critical role in the microglia-mediated neuroinflammation (Su et al. 2016).

miR-124 is expressed in microglia, where it has a role in maintaining the

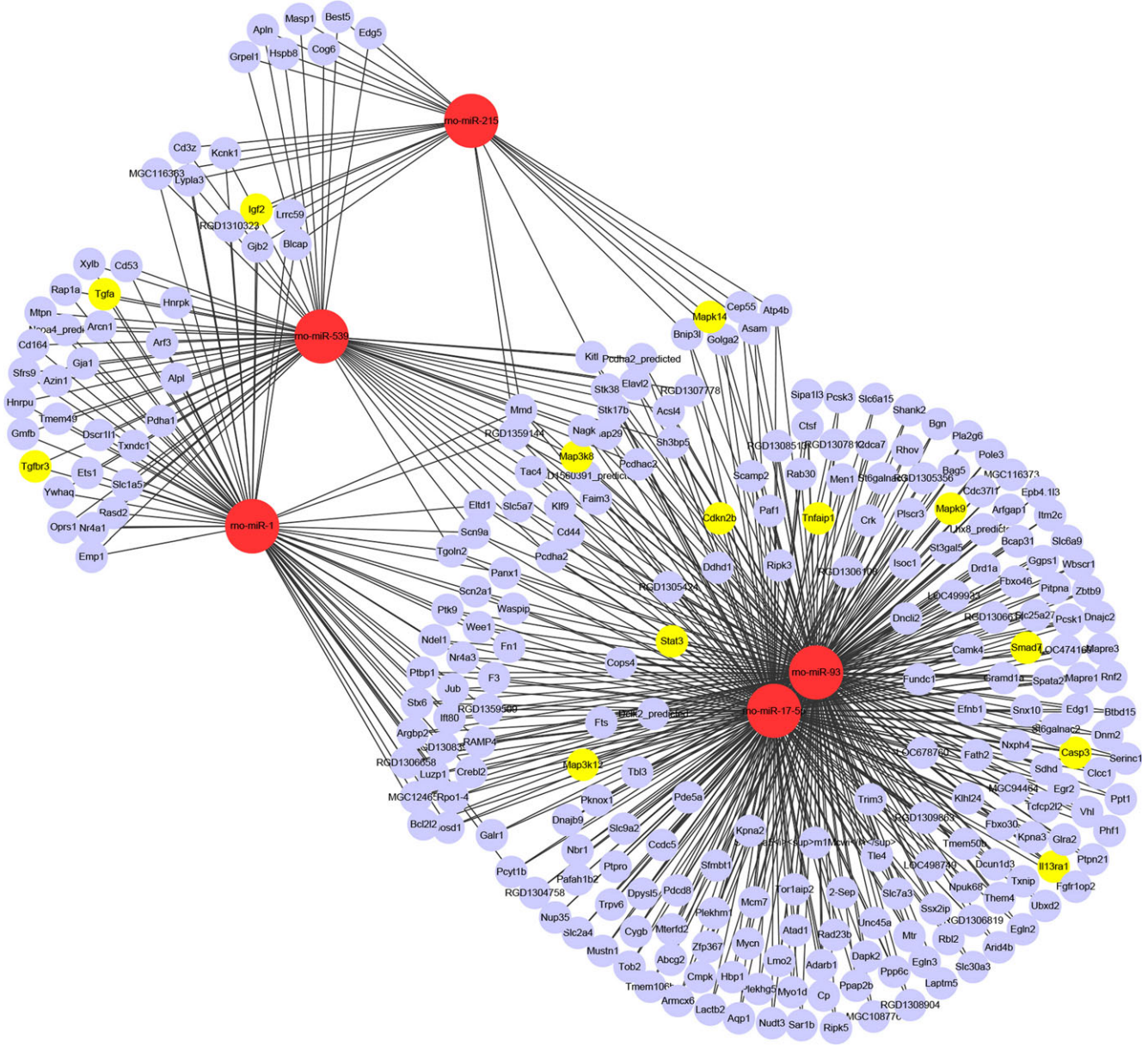

Fig. 6. Interaction network of downregulated miRNAs and their target genes. The target genes were predicted by three computational programs TARGETSCAN, MIRWALK and MIRDB. Red circles: microRNAs. Yellow circles: important target genes.

microglial cells in a quiescent state and is critical for the switching from M1 type to M2 types of retinal microglial cells (Caldeira et al. 2014). Upregulation of miR-124 may play a protective role against neural apoptosis (Sun et al. 2013). Significant upregulation of miR-124 was found in oxygen–glucose deprivation model (Kong et al. 2014). In our study, we did not detect a statistically significant change in the expression of miR-124 (Fig. 5). Because of the role of this particular miRNA in microglial quiescence, it is possible that its upregulation occurs if the increase in IOP becomes chronic. This hypothesis would explain why miR124 is not regulated in our model of AOH although it is important to have in mind that we have only examined miRNAs at 7 days after AOH, which is a limitation of the present study.

Many of the differentially expressed miRNAs are considered to modulate microglia activation and thus involved in the regulation of proinflammatory cytokines production. The target genes of miR-93-5p, one significantly downregulated miRNA in the AOH eyes, included MAPK9, MAP3K12, caspase 3 and others. MiR-93-5p has been acknowledged as a negative regulator of the immune response and can inhibit nuclear factor-kappa B (NF-κB) activation and proinflammatory cytokines (Lyu et al. 2014; Xu et al. 2014). miR-17-5p, which was detected to be downregulated in our study group, has also been considered to be a regulatory intermediate of multiple MAPKs (Cloonan et al. 2008). miR-17-5p could promote cell migration through targeting the P38 MAPK pathway (Yang et al. 2010). Moreover, overexpression of miR-17-5p was able to enhance cell proliferation by promoting G1/S transition of the cell cycle and inhibiting apoptosis in cancer cell lines (Li et al. 2015).

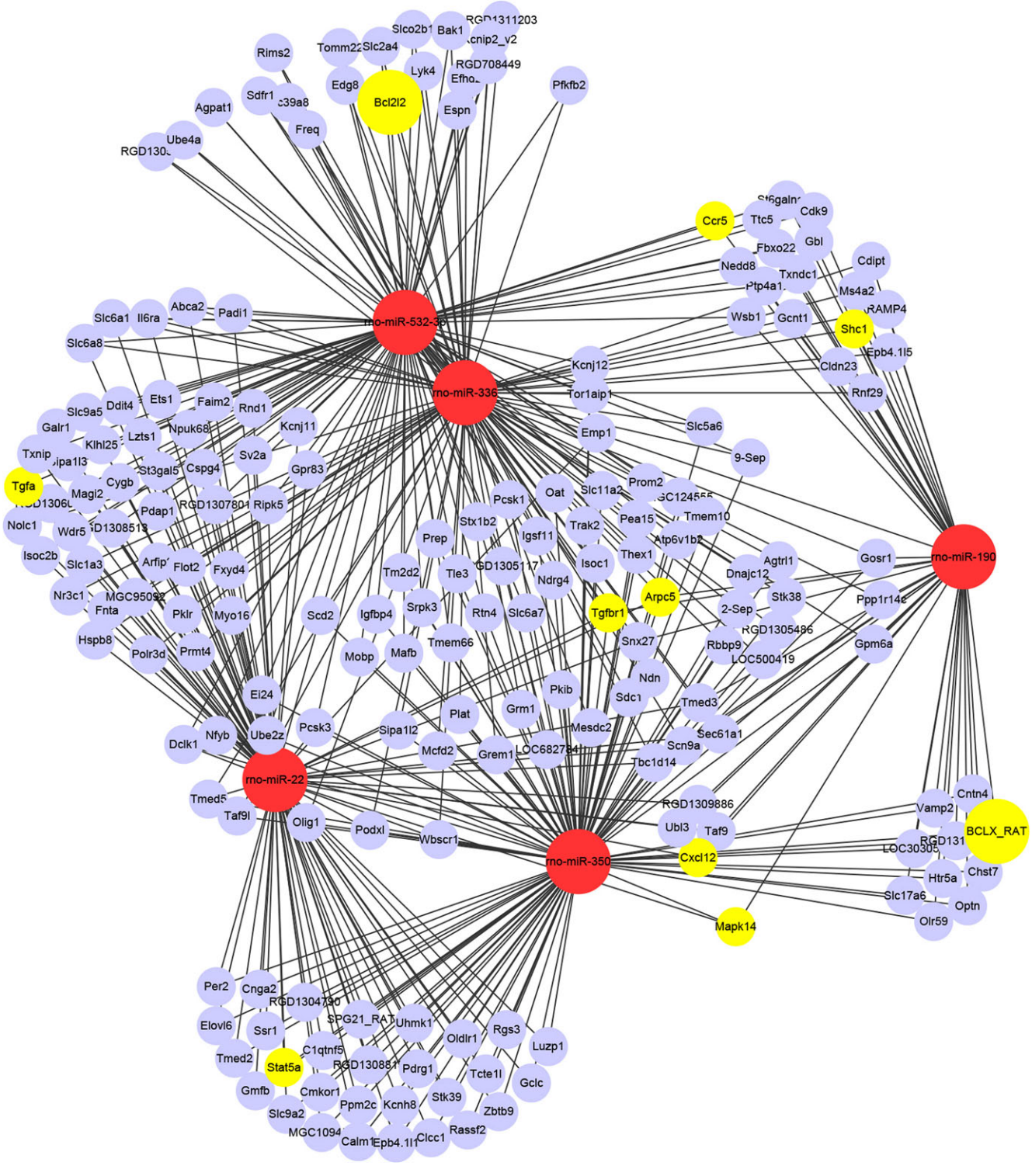

Fig. 7. Interaction network of upregulated miRNAs and their target genes. The target genes were predicted by three computational programs TARGETSCAN, MIRWALK and MIRDB. Red circles: microRNAs. Yellow circles: important target genes.

Except for the extensively studied miRNAs, some of the differentially expressed miRNAs are reported to regulate the proliferation, invasion and apoptosis of other types of cells. MiR-144, one upregulated miRNA in the acute glaucoma eyes, plays a key role in the occurrence and development of tumours, especially in the early stage of tumour formation. One of its targets is the insulin receptor substrate (IRS1) that plays important biological functions for both metabolic and mitogenic pathways and activating signalling pathways, including the PI3K pathway and the MAP kinase pathway (Joshi et al. 2005). Upregulation of miR-144 could inhibit A549 cell proliferation and reduce its invasion and migration, suggesting that miR-144 might be a tumour suppressor gene in lung cancer (Zhang et al. 2015). Therefore, we speculate that upregulation of miR-144 might be a compensatory

Table 2. Enriched signalling pathways predicted to be regulated by the downregulated miRNAs (KEGG pathway categories).

Term	Number of genes	p Value
Chemokine signalling pathway	15	0.002
Fc gamma R-mediated phagocytosis	9	0.002
MAPK signalling pathway	18	0.003
TGF-beta signalling pathway	9	0.007
GnRH signalling pathway	9	0.008
Cytokine–cytokine receptor interaction	14	0.013
Neurotrophin signalling pathway	10	0.014
SNARE interactions in vesicular transport	5	0.025
Apoptosis	9	0.036

Table 3. Enriched signalling pathways predicted to be regulated by the upregulated miRNAs (KEGG pathway categories).

Term	Number of genes	p Value
Cytokine–cytokine receptor interaction	22	0.0008
Chemokine signalling pathway	18	0.0052
Natural killer cell-mediated cytotoxicity	11	0.0280
Leucocyte transendothelial migration	12	0.0290
Cell adhesion molecules (CAMs)	14	0.0340

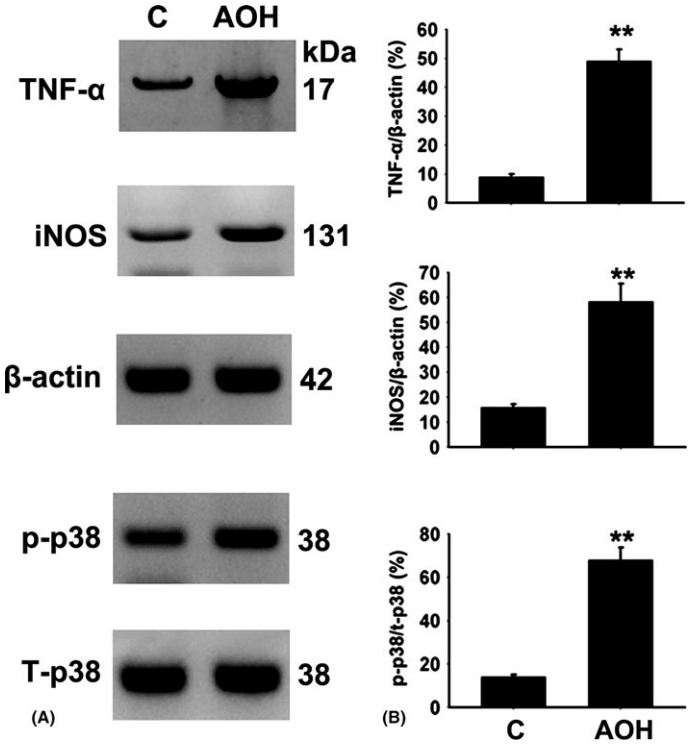

Fig. 8. Upregulation of MAPK and inflammation-related proteins. (A) Western blots from control and acute ocular hypertension retinal extracts ($n = 6$/group). TNF-α, iNOS were normalized with respect to β-actin, and the phosphorylated p38 MAP kinase (p-p38) with respect to its total (t-p38). (B) Densitometric analysis. **$p < 0.01$.

mechanism and miR-144 might also inhibit microglia activation, proliferation and migration. However, there is no related information about the function of miR-144 in the microglia cell and further study is needed in the future.

The differentially expressed miRNAs are also involved in the regulation of neural apoptosis. TGF-beta signalling pathway, neurotrophin signalling pathway and natural killer cell-mediated cytotoxicity pathway were supposed to be regulated by differentially expressed miRNAs. Some of the differentially expressed miRNAs have been considered as apoptosis-related miRNAs. MiR-592 has been thought to be a key regulator of the neurotrophin receptor p75 (NTR), which had been implicated in mediating neuronal apoptosis during injury. A previous study showed that the expression level of miR-592 decreased in neuronal ischaemic injury and overexpression of miR-592 in neurons could decrease the degree of ischaemic injury and attenuate activation of proapoptotic signalling and death in neuronal cells. Interestingly, the expression change of miR-592 in our study was highly consistent with that in focal cerebral ischaemia, which suggested that miR-592 may also influence the apoptosis of retinal ganglion cells in eyes after an acute IOP elevation (Irmady et al. 2014).

In summary, an acute IOP elevation led to changes in the expression of miRNAs, whose target genes were associated with the regulation of microglia-mediated neuroinflammation or neural apoptosis. As miRNAs are highly conserved in mammals, the findings from our investigation on rats may cautiously be transferred onto the situation in humans and may lead to a better understanding of the contribution of miRNAs to the consequences of an AOH. Addressing miRNAs in the process of retinal ischaemia and ON damage in association with high IOP may open new avenues in preventing RGC apoptosis and loss and may serve as target for future therapeutic regimen in acute glaucoma.

References

Abbott CJ, Choe TE, Lusardi TA, Burgoyne CF, Wang L & Fortune B (2014): Evaluation of retinal nerve fiber layer thickness and axonal transport 1 and 2 weeks after 8 hours of acute intraocular pressure elevation in rats. Invest Ophthalmol Vis Sci **55**: 674–687.

Almasieh M, Wilson AM, Morquette B, Cueva VJL & Di PA (2012): The molecular basis of retinal ganglion cell death in glaucoma. Prog Retin Eye Res **31**: 152–181.

Andreeva K & Cooper NG (2014): MicroRNAs in the neural retina. Int J Genomics **2014**: 165897.

Bartel DP (2004): MicroRNAs: genomics, biogenesis, mechanism, and function. Cell **116**: 281–297.

Bartel DP (2009): MicroRNAs: target recognition and regulatory functions. Cell **136**: 215–233.

Bentwich I, Avniel A, Karov Y et al. (2005): Identification of hundreds of conserved and nonconserved human microRNAs. Nat Genet **37**: 766–770.

Caldeira C, Oliveira AF, Cunha C, Vaz AR, Falcão AS, Fernandes A & Brites D (2014): Microglia change from a reactive to an age-like phenotype with the time in culture. Front Cell Neurosci **8**: 152.

Chi W, Li F, Chen H et al. (2014): Caspase-8 promotes NLRP1/NLRP3 inflammasome activation and IL-1beta production in acute glaucoma. Proc Natl Acad Sci USA **111**: 11181–11186.

Cloonan N, Brown MK, Steptoe AL et al. (2008): The miR-17-5p microRNA is a key regulator of the G1/S phase cell cycle transition. Genome Biol **9**: R127.

Dunmire JJ, Lagouros E, Bouhenni RA, Jones M & Edward DP (2013): MicroRNA in aqueous humor from patients with cataract. Exp Eye Res **108**: 68–71.

Funari VA, Winkler M, Brown J, Dimitrijevich SD, Ljubimov AV & Saghizadeh M (2013): Differentially expressed wound healing-related microRNAs in the human diabetic cornea. PLoS ONE **8**: e84425.

Galindo-Romero C, Valiente-Soriano FJ, Jiménez-López M, García-Ayuso D, Villegas-Pérez MP, Vidal-Sanz M & Agudo-Barriuso M (2013): Effect of brain-derived neurotrophic factor on mouse axotomized retinal ganglion cells and phagocytic microglia. Invest Ophthalmol Vis Sci **54**: 974–985.

Gallego BI, Salazar JJ, de Hoz R et al. (2012): IOP induces upregulation of GFAP and MHC-II and microglia reactivity in mice retina contralateral to experimental glaucoma. J Neuroinflammation **9**: 92.

Genini S, Guziewicz KE, Beltran WA & Aguirre GD (2014): Altered miRNA expression in canine retinas during normal development and in models of retinal degeneration. BMC Genom **15**: 172.

Hother C, Rasmussen PK, Joshi T et al. (2013): MicroRNA profiling in ocular adnexal lymphoma: a role for MYC and NFKB1 mediated dysregulation of microRNA expression in aggressive disease. Invest Ophthalmol Vis Sci **54**: 5169–5175.

de Hoz R, Gallego BI, Ramírez AI et al. (2013): Rod-like microglia are restricted to eyes with laser-induced ocular hypertension but absent from the microglial changes in the contralateral untreated eye. PLoS ONE **8**: e83733.

Huang Y, Li Z, van Rooijen N, Wang N, Pang CP & Cui Q (2007): Different responses of macrophages in retinal ganglion cell survival after acute ocular hypertension in rats with different autoimmune backgrounds. Exp Eye Res **85**: 659–666.

Huang Y, Cen LP, Luo JM, Wang N, Zhang MZ, van Rooijen N, Pang CP & Cui Q (2008): Differential roles of phosphatidylinositol 3-kinase/akt pathway in retinal ganglion cell survival in rats with or without acute ocular hypertension. Neuroscience **153**: 214–225.

Irmady K, Jackman KA, Padow VA et al. (2014): Mir-592 regulates the induction and cell death-promoting activity of p75NTR in neuronal ischemic injury. J Neurosci **34**: 3419–3428.

Jonas RA, Yuan TF, Liang YX, Jonas JB, Tay DK & Ellis-Behnke RG (2012): The spider effect: morphological and orienting classification of microglia in response to stimuli in vivo. PLoS ONE **7**: e30763.

Joshi MB, Philippova M, Ivanov D, Allenspach R, Erne P & Resink TJ (2005): T-cadherin protects endothelial cells from oxidative stress-induced apoptosis. FASEB J **19**: 1737–1739.

Kim EK & Choi EJ (2015): Compromised MAPK signaling in human diseases: an update. Arch Toxicol **89**: 867–882.

Kong H, Omran A, Ashhab MU et al. (2014): Changes in microglial inflammation-related and brain-enriched MicroRNAs expressions in response to in vitro oxygen-glucose deprivation. Neurochem Res **39**: 233–243.

Kovacs B, Lumayag S, Cowan C & Xu S (2011): MicroRNAs in early diabetic retinopathy in streptozotocin-induced diabetic rats. Invest Ophthalmol Vis Sci **52**: 4402–4409.

Kutty RK, Nagineni CN, Samuel W et al. (2013): Differential regulation of microRNA-146a and microRNA-146b-5p in human retinal pigment epithelial cells by interleukin-1beta, tumor necrosis factor-alpha, and interferon-gamma. Mol Vis **19**: 737–750.

Lafuente MP, Villegas-Perez MP, Selles-Navarro I, Mayor-Torroglosa S, de Imperial JM & Vidal-Sanz M (2002): Retinal ganglion cell death after acute retinal ischemia is an ongoing process whose severity and duration depends on the duration of the insult. Neuroscience **109**: 157–168.

Leung CK, Lindsey JD, Chen L, Liu Q & Weinreb RN (2009): Longitudinal profile of retinal ganglion cell damage assessed with blue-light confocal scanning laser ophthalmoscopy after ischaemic reperfusion injury. Br J Ophthalmol **93**: 964–968.

Lewis BP, Burge CB & Bartel DP (2005): Conserved seed pairing, often flanked by adenosines, indicates that thousands of human genes are microRNA targets. Cell **120**: 15–20.

Li L, He L, Zhao JL, Xiao J, Liu M, Li X & Tang H (2015): MiR-17-5p up-regulates YES1 to modulate the cell cycle progression and apoptosis in ovarian cancer cell lines. J Cell Biochem **116**: 1050–1059.

Liu N, Chen NY, Cui RX et al. (2012a): Prognostic value of a microRNA signature in nasopharyngeal carcinoma: a microRNA expression analysis. Lancet Oncol **13**: 633–641.

Liu S, Li ZW, Weinreb RN et al. (2012b): Tracking retinal microgliosis in models of retinal ganglion cell damage. Invest Ophthalmol Vis Sci **53**: 6254–6262.

Lyu X, Fang W, Cai L et al. (2014): TGFbetaR2 is a major target of miR-93 in nasopharyngeal carcinoma aggressiveness. Mol Cancer **13**: 51.

Maiorano NA & Hindges R (2012): Non-coding RNAs in retinal development. Int J Mol Sci **13**: 558–578.

Nadal-Nicolás FM, Jimenez-Lopez M, Salinas-Navarro M, Sobrado-Calvo P, Alburquerque-Béjar JJ, Vidal-Sanz M & Agudo-Barriuso M (2012): Whole number, distribution and co-expression of brn3 transcription factors in retinal ganglion cells of adult albino and pigmented rats. PLoS ONE **7**: e49830.

Nadal-Nicolás FM, Salinas-Navarro M, Jiménez-López M, Sobrado-Calvo P, Villegas-Pérez MP, Vidal-Sanz M & Agudo-Barriuso M (2014): Displaced retinal ganglion cells in albino and pigmented rats. Front Neuroanat **8**: 99.

Nadal-Nicolás FM, Sobrado-Calvo P, Jimenez-Lopez M, Vidal-Sanz M & Agudo-Barriuso M (2015): Long-term effect of optic nerve axotomy on the retinal ganglion cell layer. Invest Ophthalmol Vis Sci **56**: 6095–6112.

Naskar R, Wissing M & Thanos S (2002): Detection of early neuron degeneration and accompanying microglial responses in the retina of a rat model of glaucoma. Invest Ophthalmol Vis Sci **43**: 2962–2968.

Ortín-Martínez A, Salinas-Navarro M, Nadal-Nicolás FM et al. (2015): Laser-induced ocular hypertension in adult rats does not affect non-RGC neurons in the ganglion cell layer but results in protracted severe loss of cone-photoreceptors. Exp Eye Res **132**: 17–33.

Parrilla-Reverter G, Agudo M, Nadal-Nicolás F et al. (2009): Time-course of the retinal nerve fibre layer degeneration after complete intra-orbital optic nerve transection or crush: a comparative study. Vision Res **49**: 2808–2825.

Punj V, Matta H, Schamus S, Tamewitz A, Anyang B & Chaudhary PM (2010): Kaposi's sarcoma-associated herpesvirus-encoded viral FLICE inhibitory protein (vFLIP) K13 suppresses CXCR4 expression by upregulating miR-146a. Oncogene **29**: 1835–1844.

Rojas B, Gallego BI, Ramírez AI et al. (2014): Microglia in mouse retina contralateral to experimental glaucoma exhibit multiple signs of activation in all retinal layers. J Neuroinflammation **11**: 133.

Rovere G, Nadal-Nicolás FM, Agudo-Barriuso M, Sobrado-Calvo P, Nieto-López L, Nucci C, Villegas-Pérez MP & Vidal-Sanz M (2015): Comparison of retinal nerve fiber layer thinning and retinal ganglion cell loss after optic nerve transection in adult albino rats. Invest Ophthalmol Vis Sci **56**: 4487–4498.

Saccà SC, Gandolfi S, Bagnis A, Manni G, Damonte G, Traverso CE & Izzotti A (2016): The outflow pathway: a tissue with morphological and functional unity. J Cell Physiol **231**: 1876–1893.

Salinas-Navarro M, Alarcón-Martínez L, Valiente-Soriano FJ et al. (2009): Functional and morphological effects of laser-induced ocular hypertension in retinas of

adult albino Swiss mice. Mol Vis **15**: 2578–2598.

Salinas-Navarro M, Alarcón-Martínez L, Valiente-Soriano FJ, Jiménez-López M, Mayor-Torroglosa S, Avilés-Trigueros M, Villegas-Pérez MP & Vidal-Sanz M (2010): Ocular hypertension impairs optic nerve axonal transport leading to progressive retinal ganglion cell degeneration. Exp Eye Res **90**: 168–183.

Salvador-Silva M, Vidal-Sanz M & Villegas-Pérez MP (2000): Microglial cells in the retina of *Carassius auratus*: effects of optic nerve crush. J Comp Neurol **417**: 431–447.

Selles-Navarro I, Villegas-Perez MP, Salvador-Silva M, Ruiz-Gomez JM & Vidal-Sanz M (1996): Retinal ganglion cell death after different transient periods of pressure-induced ischemia and survival intervals. A quantitative in vivo study. Invest Ophthalmol Vis Sci **37**: 2002–2014.

Sobrado-Calvo P, Vidal-Sanz M & Villegas-Perez MP (2007): Rat retinal microglial cells under normal conditions, after optic nerve section, and after optic nerve section and intravitreal injection of trophic factors or macrophage inhibitory factor. J Comp Neurol **501**: 866–878.

Su W, Aloi MS & Garden GA (2016): MicroRNAs mediating CNS inflammation: small regulators with powerful potential. Brain Behav Immun **52**: 1–8.

Sun Y, Gui H, Li Q, Luo ZM, Zheng MJ, Duan JL & Liu X (2013): MicroRNA-124 protects neurons against apoptosis in cerebral ischemic stroke. CNS Neurosci Ther **19**: 813–819.

Tanaka Y, Tsuda S, Kunikata H et al. (2014): Profiles of extracellular miRNAs in the aqueous humor of glaucoma patients assessed with a microarray system. Sci Rep **4**: 5089.

Tuo J, Shen D, Yang HH & Chan CC (2014): Distinct microRNA-155 expression in the vitreous of patients with primary vitreoretinal lymphoma and uveitis. Am J Ophthalmol **157**: 728–734.

Valiente-Soriano FJ, Nadal-Nicolás FM, Salinas-Navarro M, Jiménez-López M, Bernal-Garro JM, Villegas-Pérez MP, Agudo-Barriuso M & Vidal-Sanz M (2015a): BDNF rescues RGCs but not intrinsically photosensitive RGCs in ocular hypertensive albino rat retinas. Invest Ophthalmol Vis Sci **56**: 1924–1936.

Valiente-Soriano FJ, Salinas-Navarro M, Jiménez-López M et al. (2015b): Effects of ocular hypertension in the visual system of pigmented mice. PLoS ONE **10**: e0121134.

Vidal-Sanz M, Bray GM, Villegas-Pérez MP, Thanos S & Aguayo AJ (1987): Axonal regeneration and synapse formation in the superior colliculus by retinal ganglion cells in the adult rat. J Neurosci **7**: 2894–2909.

Vidal-Sanz M, Salinas-Navarro M, Nadal-Nicolás FM et al. (2012): Understanding glaucomatous damage: anatomical and functional data from ocular hypertensive rodent retinas. Prog Retin Eye Res **31**: 1–27.

Vidal-Sanz M, Nadal-Nicolás FM, Valiente-Soriano FJ, Agudo-Barriuso M & Villegas-Perez MP (2015a): Identifying specific RGC types may shed light on their idiosyncratic responses to neuroprotection. Neural Regen Res **10**: 1228–1230.

Vidal-Sanz M, Valiente-Soriano FJ, Ortín-Martínez A et al. (2015b): Retinal neurodegeneration in experimental glaucoma. Prog Brain Res **220**: 1–35.

Villegas-Pérez MP, Vidal-Sanz M, Bray GM & Aguayo AJ (1988): Influences of peripheral nerve grafts on the survival and regrowth of axotomized retinal ganglion cells in adult rats. J Neurosci **8**: 265–280.

Xu Y, Jin H, Yang X, Wang L, Su L, Liu K, Gu Q & Xu X (2014): MicroRNA-93 inhibits inflammatory cytokine production in LPS-stimulated murine macrophages by targeting IRAK4. FEBS Lett **588**: 1692–1698.

Yang F, Yin Y, Wang F, Wang Y, Zhang L, Tang Y & Sun S (2010): MiR-17-5p Promotes migration of human hepatocellular carcinoma cells through the p38 mitogen-activated protein kinase-heat shock protein 27 pathway. Hepatology **51**: 1614–1623.

Zhang S, Wang H, Lu Q et al. (2009): Detection of early neuron degeneration and accompanying glial responses in the visual pathway in a rat model of acute intraocular hypertension. Brain Res **1303**: 131–143.

Zhang P, Ma Y, Wang F, Yang J, Liu Z, Peng J & Qin H (2012): Comprehensive gene and microRNA expression profiling reveals the crucial role of hsa-let-7i and its target genes in colorectal cancer metastasis. Mol Biol Rep **39**: 1471–1478.

Zhang G, An H & Fang X (2015): MicroRNA-144 regulates proliferation, invasion, and apoptosis of cells in malignant solitary pulmonary nodule via zinc finger E-box-binding homeobox 1. Int J Clin Exp Pathol **8**: 5960–5967.

Received on March 15th, 2016.
Accepted on July 10th, 2016.

Correspondence:
Xiulan Zhang MD, PhD
Glaucoma Department
Zhongshan Ophthalmic Center
State Key Laboratory of Ophthalmology
Sun Yat-Sen University
54S. Xianlie Road
Guangzhou 510060
China
Tel: +86 20 87334247
Fax: +86 20 87334645
Email: zhangxl2@mail.sysu.edu.cn
and
Manuel Vidal-Sanz, MD, PhD
Departamento de Oftalmología
Facultad de Medicina
Universidad de Murcia
Murcia 30120
Spain
Tel: +34 868884330
Fax: +34 868883962
Email: manuel.vidal@um.es

We are grateful to José Bernal-Garro for the technical support. Supported in part by the National Natural Science Foundation of China (81170849, 81371008), the Science and Technology Program of Guangdong Province, China (2013B020400003), the Science and Technology Program of Guangzhou, China (15570001) and Spanish Ministry of Economy and Competitiveness (SAF-2015-67643).